Influence of oxidized lipids on palmitoyl-oleoyl-phosphatidylcholine organization, contribution of Langmuir monolayers and Langmuir–Blodgett films

Christine Grauby-Heywang, Fabien Moroté, Marion Mathelié-Guinlet, Ibtissem Gammoudi, Ndeye Rokhaya Faye, Touria Cohen-Bouhacina

Influence of oxidized lipids on palmitoyl-oleoyl-phosphatidylcholine organization, contribution of Langmuir monolayers and Langmuir–Blodgett films

Christine Grauby-Heywang[a,*], Fabien Moroté[a], Marion Mathelié-Guinlet[a], Ibtissem Gammoudi[b], Ndeye Rokhaya Faye[a,1], Touria Cohen-Bouhacina[a]

[a] Laboratoire Ondes et Matière d'Aquitaine (LOMA), UMR CNRS 5798, Université de Bordeaux, 351 cours de la libération, 33405 Talence Cedex, France
[b] Cellule de transfert NanoPhyNov, Université de Bordeaux, 351 cours de la libération, Talence Cedex 33405, France

Keywords:
Oxidized lipid
Langmuir monolayer
Langmuir–Blodgett film
Surface pressure measurements
Atomic force microscopy

A B S T R A C T

In this work, we studied the interaction of two oxidized lipids, PoxnoPC and PazePC, with POPC phospholipid. Mean molecular areas obtained from (π A) isotherms of mixed PoxnoPC POPC and PazePC POPC monolayers revealed different behaviors of these two oxidized lipids: the presence of PoxnoPC in the monolayers induces their expansion, mean molecular areas being higher than those expected in the case of ideal mixtures. PazePC POPC behave on the whole ideally. This difference can be explained by a different conformation of oxidized lipids. Moreover the carboxylic function of PazePC is protonated under our experimental conditions, as shown by (π A) isotherms of PazePC at different pH values. Both oxidized lipids induce also an increase of the monolayer elasticity, PoxnoPC being slightly more efficient than PazePC. These monolayers were transferred from the air water interface onto mica supports for a study by AFM. AFM images are on the whole homogenous, suggesting the presence of only one lipid phase in both cases. However, in the case of PazePC POPC monolayers, AFM images show also the presence of areas thicker of 7 nm to 10 nm than the surrounding lipid phase, probably due to the local formation of multilayer systems induced by compression.

1. Introduction

Oxidation of membrane lipids can occur via different processes, such as oxidative stress responsible for the formation of reactive oxygen species (ROS) damaging biomolecules (Deigner and Hermetter, 2008), photodynamic therapies (Girotti, 2001; Castano et al., 2004) or enzymatic reactions (Greig et al., 2012). Damages due to oxidation can be dramatic, since it leads to the formation of deeply modified lipids, such as phospholipids containing hydroxyl or hydroperoxy groups on the unsaturated chain, phospholipids containing a truncated chain with a terminal carbonyl or hydroxyl group, or lysophospholipids (O'Donnel, 2011). The main conse quence of these modifications is that oxidized lipids are more polar than the intact ones. Chemically, polyunsaturated phospholipids are more sensitive to oxidation, and their polar head group is very often phosphatidylcholine (PC), PC being the major phospholipid in mammalian membranes (Catala, 2012).

Effects of these oxidized lipids are multiple. For instance, they can be recognized by specific receptors which activate different signaling pathways leading to various cellular responses (Fruh wirth et al., 2007; Greig et al., 2012). In this context, it has been shown that lipid oxidation plays a role in inflammatory processes observed in various diseases, such as atherosclerosis, cardiovascu lar diseases or cancers (Greig et al., 2012; Fruhwirth et al., 2007; Koppaka and Axelsen, 2000). Oxidized lipids could also stimulate the formation of amyloid plaques, responsible for the Alzheimer disease (Koppaka and Axelsen, 2000; Volinsky and Kinnunen,

Abbreviations: π, surface pressure; A, mean molecular area; POPC, 1-palmitoyl-2-oleoyl-sn-glycero-3-phosphocholine; OPPC, 1-oleoyl-2-palmitoyl-sn-glycero-3-phosphocholine; PoxnoPC, 1-palmitoyl-2-(9′-oxo-nonanoyl)-sn-glycero-3-phosphocholine; PazePC, 1-palmitoyl-2-azelaoyl-sn-glycero-3-phosphocholine; PC, phosphatidylcholine; PS, phosphatidylserine; ROS, reactive oxygen species; AFM, atomic force microscopy; LB, Langmuir–Blodgett.

* Corresponding author.
E-mail addresses: christine.grauby-heywang@u-bordeaux.fr (C. Grauby-Heywang), fabien.morote@u-bordeaux.fr (F. Moroté), marion.mathelie-guinlet@u-bordeaux.fr (M. Mathelié-Guinlet), ibtissem.gammoudi@u-bordeaux.fr (I. Gammoudi), rokhaya.faye@ihu-liryc.fr (N.R. Faye), touria.cohen-bouhacina@u-bordeaux.fr (T. Cohen-Bouhacina).
[1] Present address: Centre de Recherche Cardio-Thoracique de Bordeaux—INSERM U1045, IHU-LIRYC, PTIB—Hôpital Xavier Arnozan, Avenue du Haut Lévêque, 33604 Pessac, France.

2013). At last, they are involved in apoptosis, since the externali zation of oxidized lipids is necessary for the clearance of apoptotic cells by macrophages (Fruhwirth et al., 2007; Volinsky and Kinnunen, 2013).

Concerning molecular mechanisms, lipids being essential components of cells, it is clear that their oxidation can induce strong modification in the cell functioning, oxidized lipids acting as second toxic messengers or inducing structural damages in membranes (Catala, 2012; Volinsky and Kinnunen, 2013). In particular, oxidized lipids can be locally concentrated in mem branes, thus influencing their biophysical properties (Kinnunen et al., 2012; Volinsky and Kinnunen, 2013). In this context, a lot of studies have been performed on lipids from the mitochondrial membrane, since the main part of endogenous free radicals, acting as strong oxidants, is produced in mitochondria during aerobic respiration (Gabbita et al., 1998). It has been shown that the accumulation of oxidized lipids in microsomes induces an increase of the lipid acyl chain order (Eichenberger et al., 1982). In the same idea, the lipid oxidation induced by $FeSO_4$ on mitochondria decreases the membrane fluidity (Nepomuceno et al., 1997). On the contrary, Gabbita et al. observed an increase of the membrane fluidity after the oxidation of synaptosomes and mitochondrial membranes, this higher fluidity being assigned to the formation of gaps in the membranes (Gabbita et al., 1998). Disorder in the lipid packing in the presence of oxidized lipids was also reported in supported bilayers made with phospholipids from mitochondria incubated in ROS generating conditions, even if all the oxidizing conditions are not similarly efficient (Megli and Sabatini, 2003). In particular, in the case of mitochondria exposed to CCl_4, known to increase the oxidative stress in a short term, the bilayer disorder is proportional to the oxidant amount and to the incubation time (Megli and Sabatini, 2004).

However, the analysis of these experiments is difficult, since the diversity of molecules produced by oxidation in an initial complex lipid mixture is wide and the nature of oxidized molecules is not always known in details. However, perfectly defined oxidized lipids are now available, leading to less ambiguous results. This is the case of 1 palmitoyl 2 (9′ oxo nonanoyl) sn glycero 3 phos phocholine and 1 palmitoyl 2 azelaoyl sn glycero 3 phospho choline, PoxnoPC and PazePC, respectively, which are oxidized derivatives of 1 palmitoyl 2 oleoyl phosphatidylcholine or POPC. At the cellular level, it has been shown that PoxnoPC is involved in apoptosis and necrosis processes (Uhlson et al., 2002), whereas PazePC behaves as a weak ligand peroxisome receptor (Davis et al., 2001). The behavior of these lipids or similar ones included in membrane models has been already studied by different experi mental methods: electron paramagnetic resonance (Megli et al., 2005), surface pressure and surface dipole measurements coupled with fluorescence microscopy at the air water interface (Sabatini et al., 2006), fluorescence energy transfer (Mattila et al., 2008), fluorescence correlation spectroscopy z scan (Beranova et al., 2010; Parkkila et al., 2015), fluorescence solvent relaxation (Volinsky et al., 2011), scattering stopped flow experiments (Lis et al., 2011), differential scanning calorimetry and nuclear magnetic resonance (Wallgren et al., 2012; Wallgren et al., 2013) . . . Molecular simulations have been also successfully applied, giving precious complementary information, such as molecule orientation and conformation (Khandelia and Mouritsen, 2009; Beranova et al., 2010; Cwiklik and Jungwirth, 2010; Khandelia et al., 2014). On the whole, data show that oxidized lipids, in sufficient amount, can induce bilayer/micelle transitions (Megli et al., 2005), or the formation of defects and the increase of lipid flip flop (Volinsky et al., 2011). On the other hand, oxidized lipids are for instance able to stabilize sphingomyelin/cholesterol domains in ternary PC/sphingomyelin/cholesterol mixtures (Volin sky et al., 2012; Parkkila et al., 2015). Moreover, the oxidized, and thus more polar, chain is able to reverse in a more or less "extended lipid conformation" (Khandelia and Mouritsen, 2009), in order to get closer to the interfacial region or even to point out in water. This particular orientation, described recently in a "lipid whisker model" (Catala, 2012) improving the "fluid mosaic model" of Singer and Nicolson (Singer and Nicolson, 1972), induces important changes in the membrane structure and dynamics (mean molecular areas, bilayer thickness, hydration profile, phase separation . . .), depending on the percentage of the oxidized lipid, the experimental conditions (pH, cations) and the nature of surrounding lipids.

In a previous work, we studied the natural oxidation by atmospheric oxygen of Langmuir Blodgett (LB) films made of two monounsaturated lipids, POPC and OPPC (1 oleoyl 2 palmitoyl phosphatidylcholine), using atomic force microscopy (AFM) (Faye et al., 2013). AFM is a high resolution scanning probe surface analysis technique, based on the measurement of interaction forces between a fine tip and the sample surface, these forces depending on the tip sample distance. By scanning the surface it is possible to image it with lateral and perpendicular resolutions of 1 nm and 0.1 nm, respectively. To our knowledge, this powerful imaging technique has not been applied in the case of membrane systems including oxidized lipids, whereas it is perfectly adapted to the non damaging study of lipid planar monolayers and bilayers (Garcia Manyès et al., 2007; Garcia Manyès and Sanz, 2010; Faye et al., 2013). Moreover, AFM presents an important advantage as compared to widespread fluorescence microscopy, since this high resolution and non intrusive technique does not require the presence of a fluorophore, which can induce itself lipid oxidation (Ayuyan and Cohen, 2006).

AFM images of POPC and OPPC LB films showed that both films are sensitive to oxidation, even if this process is rather low and occurs after a few days. This process, which is not observed if samples are kept under vacuum, is responsible for the appearance of domains regularly distributed on the film surface and higher than the surrounding intact phase, suggesting that oxidation occurs locally, likely in areas presenting a local defect. We assumed that these domains result from the reversal of the oxidized chain, as previously described, leading to the raising of the whole molecule.

Unfortunaly, it was not possible in this first study to define the composition of LB films in terms of oxidized lipids, since this oxidation was not chemically controlled. Therefore, in the present work, we continue to explore the behavior of oxidized lipids in membrane models, by introducing PoxnoPC and PazePC, two known derivatives of POPC, in POPC monolayers. These lipids were added to POPC at a known amount (in the 4 20 mol% range). In a first step, surface pressure measurements enabled us to study the lateral packing of these lipid mixtures, whereas compressibility modulus gave information on the monolayer elasticity. As in the case of AFM, such methods have been relatively rarely applied to the study of oxidized lipids (Sabatini et al., 2006; Volinsky et al., 2012). In a second step, mixed monolayers were transferred on planar supports by the LB technique to be characterized by AFM. Our results show that PoxnoPC and PazePC behave differently in POPC monolayers in terms of mean molecular areas, PoxnoPC inducing an expansion of mixed monolayers, contrary to PazePC. Both oxidized lipids induce an increase of the monolayer elasticity. AFM images do not show any phase separation in mixed monolayers, but reveal the presence of thicker areas in LB films containing PazePC, likely due to the local formation of multilayer systems induced by compression. At last, these images are very different from those previously obtained in the case of POPC LB films submitted to atmospheric oxygen, which confirms that oxidation occurs locally and propagates by chain reaction in pure POPC LB films.

2. Material and methods

2.1. Material

PoxnoPC (1 palmitoyl 2 (9′ oxo nonanoyl) sn glycero 3 phosphocholine) and PazePC (1 palmitoyl 2 azelaoyl sn glycero 3 phosphocholine) were purchased from Avanti Polar Lipids. POPC (1 palmitoyl 2 oleoyl sn glycero 3 phosphocholine) was purchased from Sigma Aldrich. Fig. 1 shows the chemical structure of these three lipids. They were at least 99% pure and used without further purification. Chloroform and ethanol (both HPLC grade) were purchased from Sigma Aldrich. Millipore water was used as subphase (pH 5.6, resistivity higher than 18.2 MΩ cm). In the case of pure PazePC monolayers, NaOH and HCl (both from Sigma Aldrich) were occasionally added to change the subphase pH. Muscovite mica substrates for AFM experiments were purchased from Electron Microscopy Sciences (USA).

2.2. Surface pressure measurements and Langmuir Blodgett (LB) transfers

Surface pressure experiments were carried out in air, using a Nima Langmuir through (spreading surface between 40 and 234 cm^2), equipped with a Wilhelmy balance (Nima). Briefly, lipids were dissolved in a 1/1 (v/v) mixture of chloroform and ethanol at a concentration of 1 mM. In the case of mixed monolayers, appropriate volumes of each solution were mixed just before spreading, a new mixed solution being used fat each spreading. After spreading and evaporation of solvents (15 min), lipids were compressed continuously at a rate of 5 $cm^2\,min^{-1}$. During the compression, surface pressure π was measured by using a Whatman chromatography paper as Wilhelmy plate. The temperature of the room was kept constant to $20 \pm 1\,^{\circ}C$.

π A isotherms were analyzed following two complementary methods. First, averages of experimental mean molecular areas at a given surface pressure (obtained from several isotherms realized independently) were compared to theoretical ones, obtained at the same pressure from the addition of mean molecular areas of single components taking into account their mole fraction (Gaines, 1966). Secondly the reciprocal isothermal compressibility C_S^{-1} (compressibility modulus) was determined from the compressibility $C_S = (-1/A_\pi) \times (dA/d\pi)$ where A_π is the mean molecular area at a given surface pressure π. A high C_S^{-1} value is indicative of a low interfacial elasticity.

Monolayers were transferred from the air water interface onto freshly cleaved mica by the LB method, by using a dip coated mechanism from Nima. Mica was first immersed in water, perpendicularly to the interface, and the lipid monolayer was spread as previously described and compressed until a surface pressure of 30 $mN.m^{-1}$. This surface pressure was next kept constant thanks to a control system maintaining the pressure by adjusting the surface occupied by the monolayer. After stabilization of the lipid monolayer (a few minutes at most), mica was removed from water at a rate of 5 $mm\,min^{-1}$, and kept protected from dust until its imaging by AFM in the following hours.

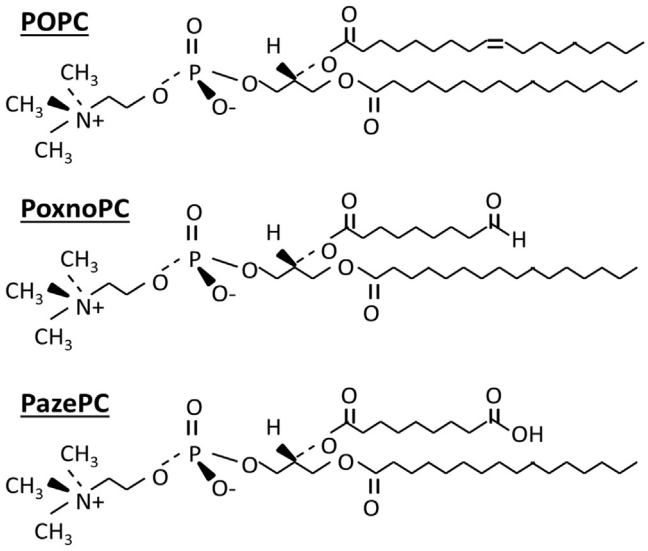

Fig. 1. Chemical structures of POPC, PoxnoPC and PazePC.

2.3. Atomic force microscopy

AFM images were recorded with a BioscopeII AFM setup (Veeco Brucker, Santa CA) equipped with a G scanner (maximum XYZ scan range of $150\,\mu m \times 150\,\mu m \times 12\,\mu m$). Samples were scanned in tapping mode using PPP NCL silicon probes (NANO SENSORS™) with a spring constant of about $32\,N\,m^{-1}$ and a corresponding measured resonance frequency of about 165 kHz. All scans were done at air and room temperature ($20 \pm 1\,^{\circ}C$) with scan rates between 0.3 Hz and 1 Hz (according to the scan size and the scanning mode). Samples were scanned in the hours following the monolayer deposition in order to avoid any damages due to oxidation (Faye et al., 2013). Three similar LB films were systematically studied to ensure reproducibility, and different areas of each sample were observed. AFM data were processed using the Nanoscope (version 7.30, Veeco) and the Gwiddion softwares.

3. Results

Fig. 2A shows the π A isotherms of PoxnoPC, POPC and their mixtures containing from 4 to 20 mol% of PoxnoPC. Isotherms of PoxnoPC and POPC are in agreement with those previously described (Sabatini et al., 2006; Lai et al., 1994; Grechishnikova et al., 1999), and suggest that these lipids are in liquid expanded phase, as their mixtures. The collapse surface pressure for PoxnoPC is rather low, around 31 $mN\,m^{-1}$, but the presence of POPC into the monolayers increases their stability at high pressure.

Experimental mean molecular areas (A_{exp}) of mixed monolayers have been compared to ideal ones defined as $A_{ideal-mixture} = X_1A_1 + (1 - X_1)A_2$, where A_1 and A_2 are the mean molecular areas of lipids *1* and *2* at a given surface pressure, and X_1 the mole fraction of the lipid *1* in the monolayer (Gaines, 1966). Any deviation $\Delta A = A_{exp} - A_{ideal-mixture} \neq 0$ from this expression indicates that the mixture is not ideal because of attractive or repulsive forces between the two molecules, inducing the condensation ($\Delta A < 0$) or the expansion ($\Delta A > 0$) of the mixed monolayers, respectively. It also provides evidence for molecular miscibility (Gaines, 1966).

However, this analysis makes sense only if uncertainties in mean molecular areas deduced from π A isotherms are weak. In the case of pure POPC monolayers, π A isotherms were reproducible with typical variations of mean molecular area around 1.5 $Å^2$ in the surface pressure range of 5 – 30 $mN\,m^{-1}$. In the same surface pressure range, variations of mean molecular areas were around 2.5 – 3.5 $Å^2$ in the case of PazePC, and 1.5 – 2.0 $Å^2$ in the case of PoxnoPC, uncertainties for corresponding mixed monolayers being in the same range.

The analysis of mean molecular areas of mixed PoxnoPC POPC monolayers at different surface pressures shows that they are higher than those expected in ideal mixtures, ΔA values ranging

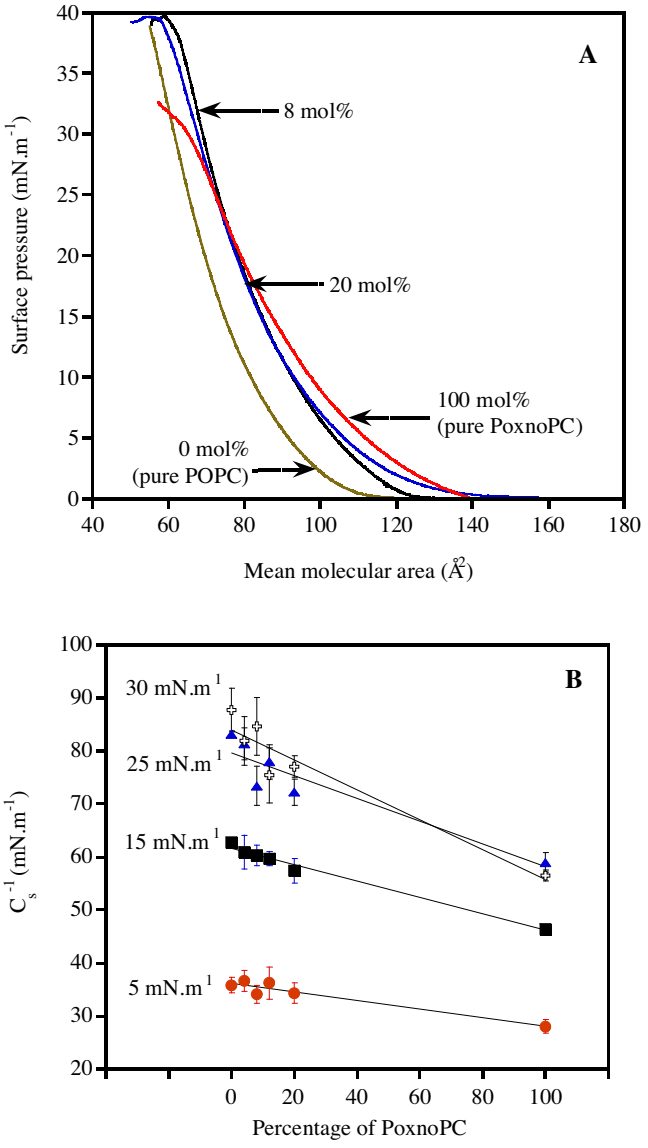

Fig. 2. (A) π–A isotherms of PoxnoPC, POPC and their mixtures (subphase ultrapure water pH 5.6, T = 20 ± 1 °C, compression speed 5 cm^2 min^{-1}). Percentages of PoxnoPC are indicated. (B) Compressibility modulus C_S^{-1} versus the percentage of PoxnoPC into mixed monolayers (average values obtained from several independent isotherms). Straight lines are added to guide the eye.

from 4.0 to 6.5 Å^2 according to the surface pressure and the amount of PoxnoPC. In all cases, the amplitude of the expansion decreases when the surface pressure increases. The expansion of PoxnoPC POPC monolayers suggests that molecules are at least partly miscible.

At last, Fig. 2B shows the variation of the compressibility modulus C_S^{-1} versus the percentage of PoxnoPC into the monolayer. Pure PoxnoPC monolayer is characterized by C_S^{-1} values roughly between 30 and 60 mN m^{-1} in the surface pressure range of 5 30 mN m^{-1}. These values are in agreement with those previously reported by Sabatini and coworkers for this lipid (Sabatini et al., 2006). Compressibility modulus logically increases when surface pressure increases, showing the decrease of the monolayer elasticity. Taking into account the experimental uncertainty on this parameter, it gets to a constant value for surface pressure above 20 mN m^{-1}. In the case of POPC, values of compressibility modulus are consistent with those previously reported (Li et al., 2001; Matti et al., 2001). At last, in the case of mixed PoxnoPC POPC monolayers, the variation of compressibility modulus with surface pressure is similar, an increase of the PoxnoPC amount into the monolayer increasing its elasticity. On the whole, a similar variation was observed in the case of PoxnoPC DPPC monolayers studied by Sabatini and coworkers, with higher C_S^{-1} values due to the higher rigidity of DPPC as compared to POPC one (Sabatini et al., 2006).

Monolayers were then transferred on mica at 30 mN m^{-1} to be observed by AFM. This surface pressure is close from the surface pressure of PoxnoPC collapse, but this value corresponds to the estimated membrane surface pressure (Janmey and Kinnunen, 2006). Moreover, a sufficiently high surface pressure is required to keep lipid cohesion (more particularly in the case of fluid POPC), and the presence of POPC in mixed monolayers increases the collapse surface pressure, as shown in Fig. 2A. Fig. 3A shows the AFM image of a pure PoxnoPC LB film. The film appears homogenous, with an average surface roughness of 0.1 nm, in agreement with the fact that this lipid is in an expanded phase. We observed previously the same feature with POPC LB films (Faye et al., 2013). Fig. 3B shows an image of a PoxnoPC POPC LB film containing 20 mol% of PoxnoPC. This uniform image (average surface roughness around 0.2 nm) suggests that PoxnoPC is homogenously distributed in POPC (similar images were obtained at other mol% of PoxnoPC with a comparable surface roughness, or at lower scale, data not shown).

In the case of PazePC, an important point is first to determine if the carboxylic function of the oxidized chain is protonated or not under our experimental conditions. Fig. 4A shows the (π A) isotherm of PazePC spread on ultrapure water. This isotherm is in agreement with those previously reported (Sabatini et al., 2006; Volinsky et al., 2012) and shows that this lipid is in expanded phase as PoxnoPC, with mean molecular areas shifted to higher values (around 10 Å^2). It has been reported that the pKa value of the carboxylic function of the oxidized chain is unusually high in the 7 8 range (Nagle et al., 2013). This unusual range is supported by a study of the cytochrom *c* PazePC interaction using quenching of pyrene emission (Mattila et al., 2008): the electrostatic interaction decreases when pH decreases from 7.4 to 5.0, because of PazePC protonation at low pH. These results suggest that PazePC carboxylic function is protonated under our experimental con ditions. However, to confirm this hypothesis, (π A) isotherms of PazePC were also performed on water subphase at pH 3.0 and 10.0 (Fig. 4B). Isotherm obtained at acidic pH is similar to the one obtained with ultrapure water, whereas isotherm obtained at basic pH is clearly different: in this case, compression induces also a regular increase of surface pressure but with a different slope. Compressibility modulus was determined at various surface pressures for all pH values: in the case of PazePC monolayers spread on pure water, they are in the same range than the compressibility of PoxnoPC monolayers, but slightly higher, increasing from 30 mN m^{-1} to 75 mN m^{-1} when surface pressure increases from 5 mN m^{-1} to 30 mN m^{-1}. They are on the whole in the same range if the pH of the subphase is acidic, but clearly lower at basic pH (around 25 30 mN m^{-1} at a surface pressure of 10 mN m^{-1} for instance). Moreover, at surface pressure higher than 15 mN m^{-1}, the isotherm bends in a potential phase transition. Surface of the through being too small to further compress the monolayer, the same experiment was repeated with a higher number of spread molecules. Even under these new conditions it was not possible to compress the monolayer above a surface pressure of 20 22 mN m^{-1}, suggesting that the monolayer is unstable. Finally, we can conclude from these results that PazePC carboxylic function is mainly protonated when it is spread on ultrapure water, since (π A) isotherm is similar to the one

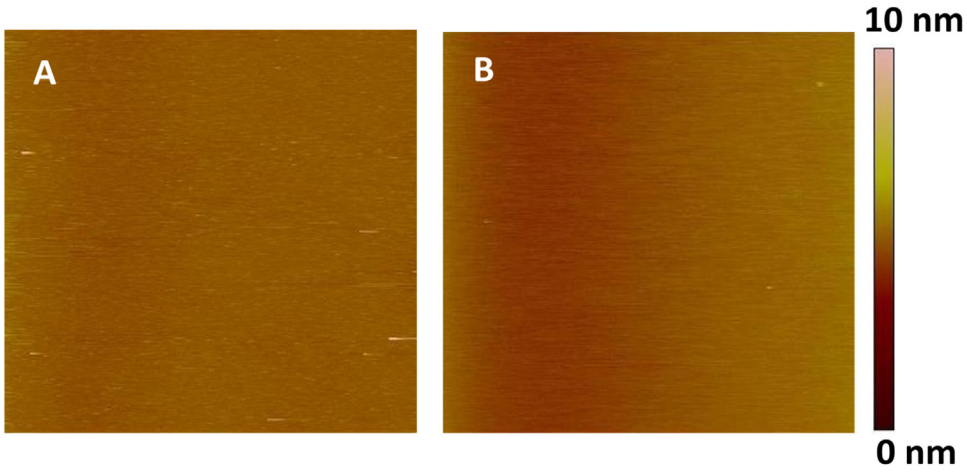

Fig. 3. (A) Height AFM images ($30 \times 30\ \mu m^2$) of a pure PoxnoPC LB film. (B) Height AFM image ($30 \times 30\ \mu m^2$) of a mixed PoxnoPC (20 mol%)–POPC LB film. Both films are transferred at 30 mN m ^{1}.

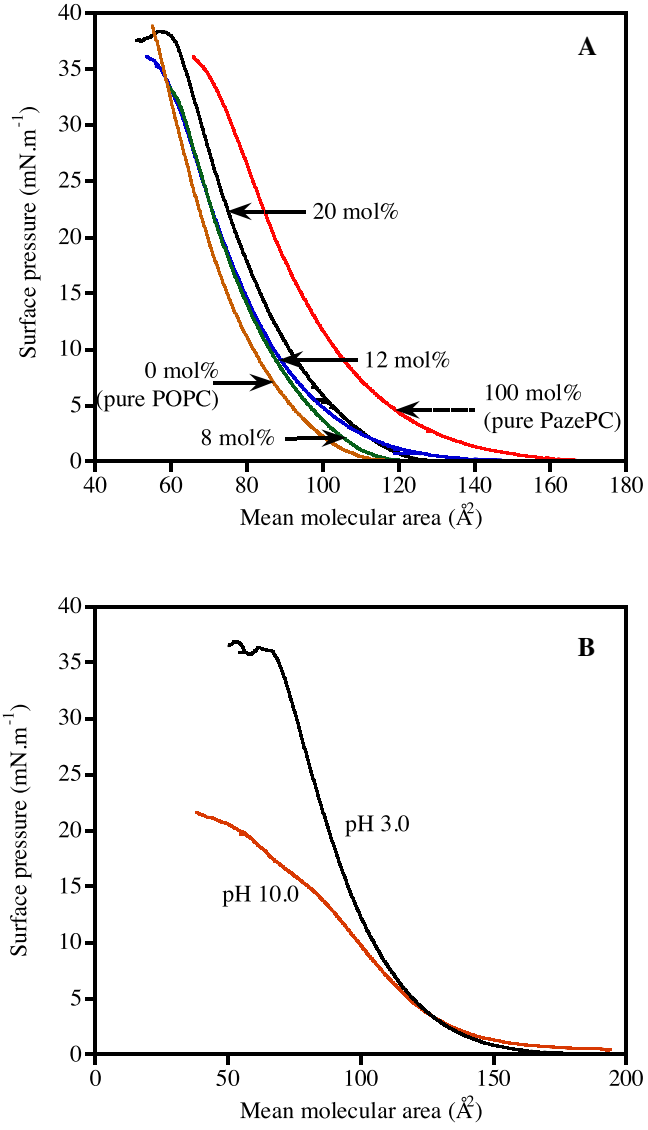

Fig. 4. (A) π–A isotherms of PazePC, POPC and their mixtures (subphase ultrapure water pH 5.6, T = 20 ± 1 °C, compression speed 5 cm^2 min ^{1}). Percentages of PazePC are indicated. (B) π–A isotherms of PazePC on ultrapure water at pH 3.0 and 10.0 (T = 20 ± 1 °C, compression speed 5 cm^2 min ^{1}).

obtained at pH 3.0. The instability of the monolayer at pH 10.0, likely due to electrostatic repulsion, confirms this hypothesis.

Mixed monolayers (POPC + 4 to 20 mol% of PazePC) are also in an expanded phase, but contrary to the case of PoxnoPC, the presence of POPC does not change significantly the stability of monolayers at high surface pressure, collapse occurring in the same range of surface pressure values. The analysis of mean molecular areas shows a modest expansion of the monolayers in the presence of PazePC (data not shown), but ΔA values are in the range of experimental errors, leading to the final conclusion that these mixtures would rather behave as ideal ones. As indicated previously, compressibility modulus of pure PazePC monolayers is slightly higher than those of PoxnoPC monolayers. This shows that PazePC monolayers are slightly less elastic. In the case of PazePC POPC mixed monolayers, an increase of PazePC percentage increases the monolayer elasticity but in a slightly weaker manner than PoxnoPC (data not shown).

PazePC forms homogenous films with an average surface roughness of 0.1 nm (data not shown), in agreement with its expanded phase. In the case of PazePC POPC LB films, height and phase AFM images (Fig. 5A and B) are on the whole also uniform (average surface roughness around 0.1 nm), but it is possible to observe small areas characterized by a higher thickness usually from 7 nm to 10 nm above the homogenous surrounding phase as shown by height profiles extracted from height image (Fig. 5C). The contrast observed in phase image (Fig. 5B) suggests a different molecular organization between the homogenous surrounding phase and protrusions, the phase difference between both areas being in a range of 50 55°, commonly met in the case of lipids. At last, typical dimensions of these structures are in the 70 100 nm range, the biggest ones having dimension around 500 nm. Their density into LB films increases with the percentage of PazePC in the monolayer, and they are not observed if the monolayer is transferred at 20 mN m ^{1} instead of 30 mN m ^{1} (data not shown).

4. Discussion

Surface pressure measurements show that PoxnoPC and PazePC are both in a liquid expanded phase, PazePC π A isotherm being shifted to higher mean molecular areas as compared to the PoxnoPC one. AFM images of corresponding LB films confirms the presence of only one phase for both lipids at the lateral resolution of the AFM setup (around 1 nm).

It has been proposed thanks to molecular simulations that polar oxidized chains are able to orientate more or less parallel to the

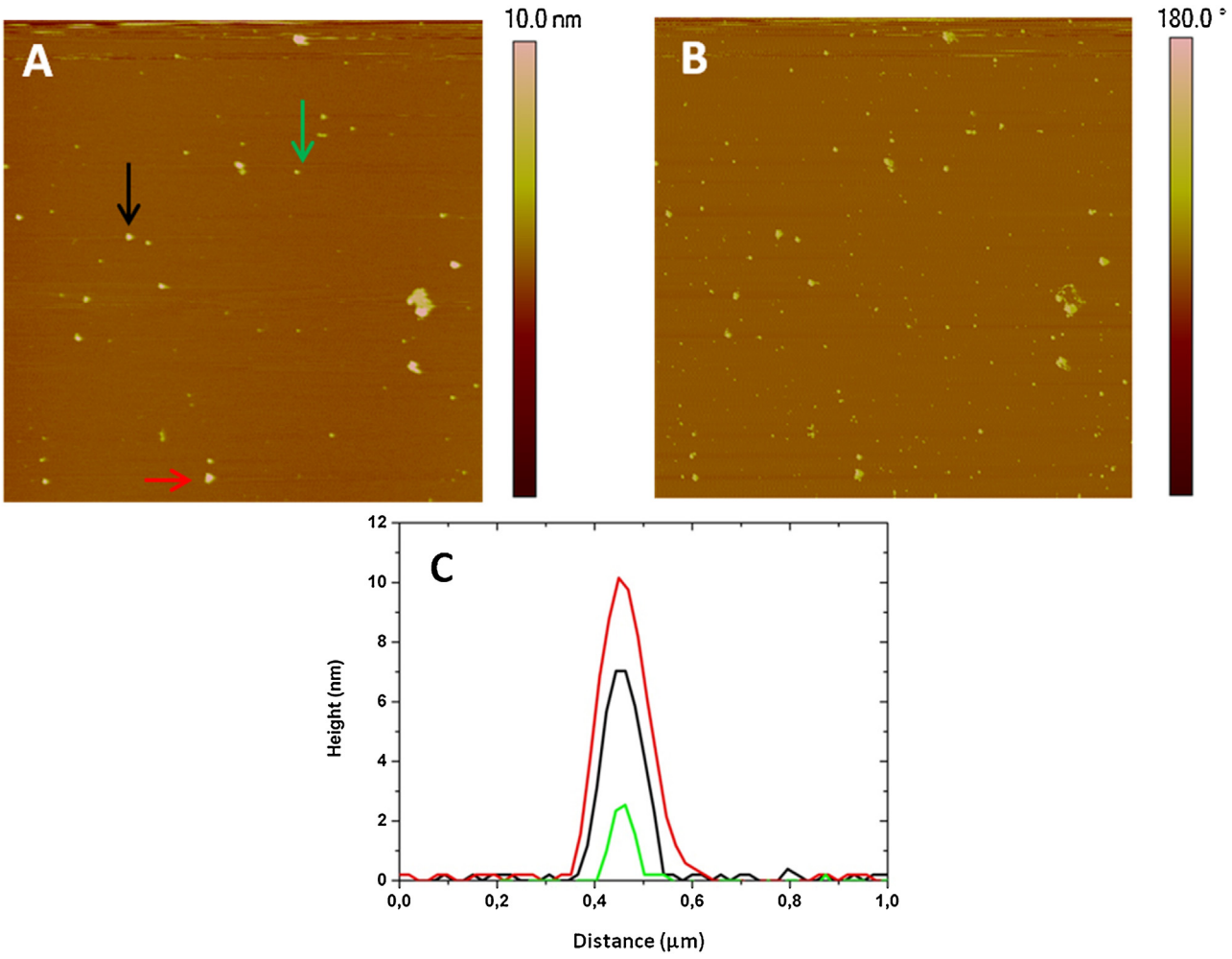

Fig. 5. (A) Height AFM image ($10 \times 10\ \mu m^2$) of a mixed PazePC (20 mol%)-POPC LB film transferred at 30 mN m ^{1}. (B) Corresponding phase image. (C) Height profiles obtained from sections indicated in the image of PazePC–POPC LB film.

air water interface or even to plunge into water with an extended conformation. The oxidized chain of PazePC being more polar than the chain of PoxnoPC, the extended conformation is favored (Khandelia and Mouritsen, 2009). This result is in contradiction with higher mean molecular areas observed on our isotherms, since an extended conformation would rather favor a gathering of molecules into the monolayer during compression. Moreover, the reversal of the oxidized chain of PazePC is favored by the deprotonation of the COOH group at the end of this chain, leading to a higher affinity of this part of the molecule for water. Under our experimental conditions, the carboxylic function of the oxidized chain is protonated as shown by experiments performed at different pH values and in agreement with its expected pKa value around 7 8 (Nagle et al., 2013). This leads to the conclusion that the higher mean molecular areas observed on (A) isotherm of PazePC are probably not due to electrostatic repulsion, carboxylic function on the oxidized chain being neutral. At last, taking into account the fact that this function in the protonated form is stable in lipid bilayers as shown by simulations on Glu and Asp amino acids (MacCallum et al., 2008), the carboxylic function is likely embedded in lipid and the oxidized chain not reversed. In the case of PoxnoPC, a partial reversal, or at least a tilt of the chain as compared to monolayer normal, is not excluded.

A isotherms of lipid mixtures suggest that they are in a liquid expanded phase under our experimental conditions. Analysis of mean molecular areas and compressibility modulus of mixed monolayers shows that the presence of PoxnoPC induces their expansion and increases the monolayer elasticity. These results can be partly compared to those obtained by Sabatini and coworkers (Sabatini et al., 2006), who studied monolayers of DPPC containing PoxnoPC. They observed that this lipid induces an expansion of the monolayers until a surface pressure around 20 mN m ^{1}, coupled with the gradual disappearance of the phase transition of DPPC and an increase of the film elasticity. AFM images of PoxnoPC POPC LB films are homogenous, suggesting that PoxnoPC is regularly distributed in the monolayers, in agreement with the expansion (Gaines, 1966).

As previously mentioned, simulations showed that the oxidized chain of PoxnoPC is able to lie more or less parallel to the interface, expanding the monolayer of a few Å^2 (Khandelia and Mouritsen, 2009). In the case of PoxnoPC DPPC monolayers studied by Sabatini and coworkers, the expansion is in the same range, except at a surface pressure of 10 mN m ^{1} where expansion is higher (around 10 Å^2). Expansion observed in the case of PoxnoPC POPC monolayers (between 4.0 and 6.5 Å^2) are in agreement with these previous results, even if no clear correlation has been observed between the amplitude of the expansion and the percentage of PoxnoPC contrary to the case of DPPC (it could be due to different parameters such as different orientations of the oxidized chain in the same sample combined with the high fluidity of POPC).

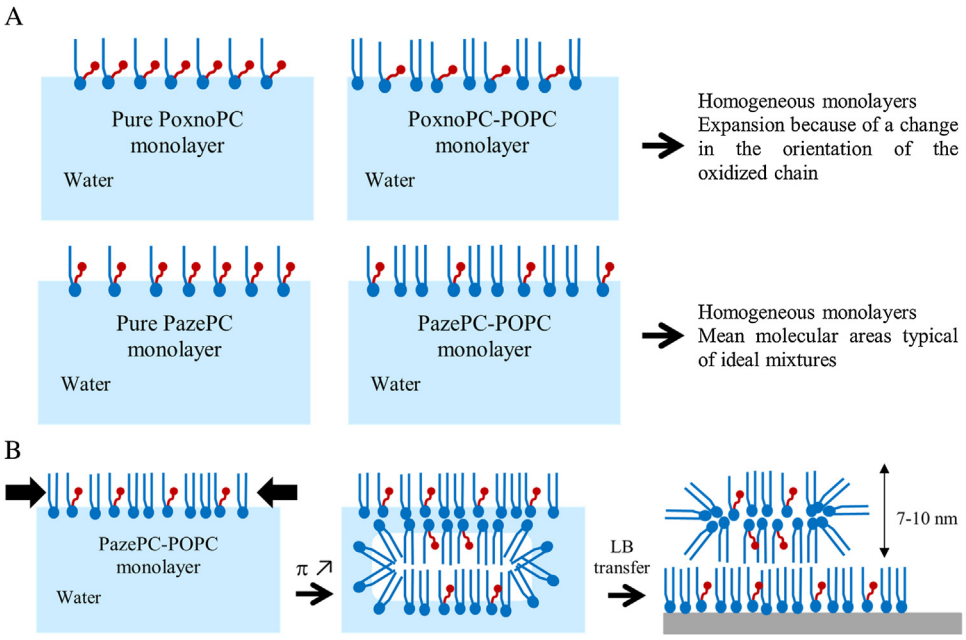

Fig. 6. (A) Scheme summarizing the organization of PoxnoPC and PazePC in pure and mixed monolayers, deduced from surface pressure measurements and AFM; (B) Scheme of a possible organization of lipids in PazePC–POPC LB films, with the formation of multilayer systems induced by compression, raising above the level of the LB film during the transfer of the monolayer from the air–water interface.

Moreover, it suggests that the oxidized chain is more tilted as compared to the monolayer normal in the presence of POPC as schematically shown in Fig. 6A, since a similar orientation would not cause an expansion. It also explains the higher compressibility of mixed monolayers.

Results are different in the case of PazePC POPC monolayers, even if PazePC increases also the monolayer elasticity (in a lower extend than PoxnoPC). As mentioned in the results, we assume that these mixtures behave ideally according to the definition of Gaines (Gaines, 1966). In the case of ideal mixtures, either lipids are miscible without interaction, or they form separated phases. Assuming that oxidized chains of PazePC molecules remain embedded in the plane of the monolayer without reversal (carboxylic groups being protonated), both hypotheses are possible if we suppose that the overall molecular organization remains the same between pure and mixed monolayers.

Under these conditions, AFM is a pertinent tool to understand the behavior of PazePC in PazePC POPC LB films. Corresponding images are on the whole homogenous, at least at surface pressure lower than 30 mN m ^{1}, suggesting a mainly homogenous distribu tion of both lipids. However, images also reveal the presence of areas thicker than the surrounding phase, the thickness ranging on the whole from 7 to 10 nm. These areas are probably due to the local formation of multilayer systems beneath the monolayer induced by compression (the monolayer transfer inducing the elevation of these multilayer systems above the surface of the LB film, as sketched in Fig. 6B). Such structures appear probably during the time where the surface pressure is kept constant (just before and during the transfer), since no sign is visible in π A isotherms and in C_S ^{1} measurements. However, some irregulari ties in the overall linear decrease with time of the surface occupied by the monolayer are observed during the transfer (data not shown). Such irregularities could be the sign of adjustments in the monolayer. Moreover the simultaneous presence of both lipids is necessary to observe these multilayer systems, since they are not observed in the case of single component LB films. These areas are either not observed if the LB film is transferred at a lower surface pressure, and their density into the LB film increases when the percentage of PazePC increases.

Taking into account the average length of a lipid molecule around 2 3 nm (Enders et al., 2004; Kucerka et al., 2005; Roiter et al., 2009; Orsi et al., 2010), the thickness range of these areas suggests that up to five monomolecular layers could be super imposed locally under the monolayer at the air water interface. Moreover, the phase signal in AFM being sensitive, in the case of soft materials, to the viscoelastic properties and adhesion forces, phase images can thus be linked to dissipative processes. In our case, contrast in the phase image (Fig. 5B) suggests a different molecular organization between the two kinds of areas, one made of lipid organized in a homogenous monolayer (dark ones) and one made of more organized/rigid molecules (bright ones).

These observations are once again partly in agreement with the study of Sabatini and coworkers (Sabatini et al., 2006), who noted an apparent condensation of DPPC monolayers containing PoxnoPC and PazePC at surface pressures above 45 mN m ^{1}, due in fact to the dissolving of oxidized lipids and micelle formation. They also suggested that the monolayer areas where dissolving occurs could be small enough that the surrounding matrix would retain oxidized lipids. Our results confirm this hypothesis, at least in the case of PazePC, since the multilayer systems observed by AFM do not detach from the monolayer. Moreover height sections performed on AFM images enable also to estimate the mean diameter of such areas around a few hundreds of nm. Micelle formation has also been proposed in ternary lipid mixtures containing high percentages of oxidized lipids (Megli et al., 2005). At last, the fact that we do not observe such protrusions in PoxnoPC POPC monolayers could be due to the fact that required experimental conditions to observe them would be slightly different, for instance in terms of surface pressure.

Finally, both oxidized lipids are miscible with POPC. This miscibility confirms results of a previous study by electron paramagnetic resonance of lipid vesicles containing oxidized lipids suggesting that fluid membranes would be protected against phase separation (Megli et al., 2005). This protection is likely due

to the fact that POPC is a fluid lipid, able of adjustment at the root of only one phase. On the contrary, the study by fluorescence microscopy of DPPC monolayers containing PoxnoPC or PazePC shows a phase separation, with domains made of DPPC in the liquid condensed phase remaining into the monolayers, even if their size and shape are modified (Sabatini et al., 2006). In the same idea, the addition of PazePC to POPC POPE cardiolipin mixtures induces a broadening of the heat profile obtained by differential scanning calorimetry, suggesting the presence of PazePC rich and PazePC poor domains (Wallgren et al., 2012). A phase separation was also observed in the case of DMPC vesicles containing either PazePC or PoxnoPC, the effect of oxidized lipids being visible event at a very low percentage of 2 mol% (Wallgren et al., 2013).

At last, AFM images of mixed monolayers are clearly different from those obtained in the case of POPC LB films oxidating "naturally" in the presence of oxygen, showing the appearance with time of domains regularly distributed (Faye et al., 2013). This difference confirms our previous hypothesis, based on the local oxidation of POPC molecules and the oxidation propagation.

5. Conclusion

This work shows that coupling surface pressure measurements and AFM imaging of transferred LB films is a powerful approach to better understand the behavior of oxidized lipids in membrane models. This combination enabled us to confirm the miscibility of PoxnoPC and PazePC in POPC monolayers, even if these oxidized lipids do not have probably the same conformation. At last, AFM showed, at least in the case of PazePC, the formation of thicker areas suggesting the local formation of multilayer systems beneath the monolayer.

Acknowledgements

We thank the Région Aquitaine and CNRS (France) for supporting this work through the Ph.D. grant of N.R. Faye and the equipment of the NanoSpectroImagerie (NSI LOMA) platform used in this work. We also thank the Direction Générale de l'Armement (DGA, Ministère de la Défense, France) and the Région Aquitaine (France) for the Ph.D. grant of M. Mathelié Guinlet.

References

Ayuyan, A.G., Cohen, F.S., 2006. Lipid peroxides promote large rafts: effects of excitation of probes in fluorescence microscopy and electrochemical reactions during vesicle formation. Biophys. J. 91, 2172–2183.
Beranova, L., Cwiklik, L., Jurkiewicz, P., Hof, M., Jungwirth, P., 2010. Oxidation changes physical properties of phospholipid bilayers: fluorescence spectroscopy and molecular simulations. Langmuir 26, 6140–6144.
Castano, A.P., Demidova, T.N., Hamblin, M.R., 2004. Mechanisms in photodynamic therapy: part one-photosensitizers, photochemistry and cellular localization. Photodiagnosis Photodyn. Ther. 1, 279–293.
Catala, A., 2012. Lipid peroxidation modifies the picture of membranes from the fluid mosaic model to the lipid whisker model. Biochimie 94, 101–109.
Cwiklik, L., Jungwirth, P., 2010. Massive oxidation of phospholipid membrane leads to pore creation and bilayer disintegration. Chem. Phys. Lett. 486, 99–103.
Davis, S.S., Pontsler, A.V., Marathe, G.K., Harrison, K.A., Murphy, R.C., Hinshaw, J.C., Prestwich, G.D., St Hilaire, A., Prescott, S.M., Zimmerman, G.A., McIntyre, T.M., 2001. Oxidized alkyl phospholipids are specific, high affinity peroxisome proliferator-activated receptor γ ligands and agonists. J. Biol. Chem. 276, 16015–16023.
Deigner, H.-P., Hermetter, A., 2008. Oxidized phospholipids: emerging lipid mediators in pathophysiology. Curr. Opin. Lipidol. 19, 289–294.
Eichenberger, K., Böhni, P., Winterhalter, K.H., Kawato, S., Richter, C., 1982. Microsomal lipid peroxidation causes an increase in the order of the membrane lipid domain. FEBS Lett. 142, 59–62.
Enders, O., Ngezahayo, A., Wiechmann, M., Leisten, F., Kolb, H.-A., 2004. Structural calorimetry of main transition of supported DMPC bilayers by temperature-controlled AFM. Biophys. J. 87, 2522–2531.
Faye, N.R., Moroté, F., Grauby-Heywang, C., Cohen-Bouhacina, T., 2013. Oxidation of Langmuir–Blodgett films of monounsaturated lipids studied by atomic force microscopy. Int. J. Nanotechnol. 390–403 (5/6/7).
Fruhwirth, G.O., Loidl, A., Hermetter, A., 2007. Oxidized phospholipids: from molecular properties to disease. Biochim. Biophys. Acta 1772, 718–736.
Gabbita, S.P., Subramaniam, R., Allouch, F., Carney, J.M., Butterfield, D.A., 1998. Effects of mitochondrial respiratory stimulation on membrane lipids and proteins: an electron paramagnetic resonance investigation. Biochim. Biophys. Acta 1372, 163–173.
Gaines, G.L., 1966. Mixed monolayers. In: Prigogine, I. (Ed.), From Insoluble Monolayers at Liquid–Gas Interfaces. Intersciences Publishers, pp. 81–300.
Garcia-Manyès, S., Sanz, F., 2010. Nanomechanics of lipid bilayers by force spectroscopy with AFM: a perspective. Biochim. Biophys. Acta 1798, 741–749.
Garcia-Manyès, S., Domenèch, O., Sanz, F., Montero, M.T., Hernandez-Borrel, J., 2007. Atomic force microscopy and force spectroscopy study of Langmuir–Blodgett films formed by heteroacid phospholipids of biological interest. Biochim. Biophys. Acta 1768, 1190–1198.
Girotti, A.W., 2001. Photosensitized oxidation of membrane lipids: reaction pathways, cytotoxic effects, and cytoprotective mechanisms. J. Photochem. Photobiol. B 63, 103–113.
Grechishnikova, I.V., Bergström, F., Johansson, L., Brown, R.E., Molotkovsky, J.G., 1999. New fluorescent cholesterol analogs as membrane probes. Biochim. Biophys. Acta 1420, 189–202.
Greig, F.H., Kennedy, S., Spickett, C.M., 2012. Physiological effects of oxidized phospholipids and their cellular signaling mechanisms in inflammation. Free Radic. Biol. Med. 52, 266–280.
Janmey, P.A., Kinnunen, P.K.J., 2006. Biophysical properties of lipids and dynamic membranes. Trends Cell Biol. 16, 538–546.
Khandelia, H., Mouritsen, O.G., 2009. Lipid gymnastics: evidence of complete acyl chain reversal in oxidized phospholipids from molecular simulations. Biophys. J. 96, 2734–2743.
Khandelia, H., Loubet, B., Olzynska, A., Jurkiewics, P., Hof, M., 2014. Pairing of cholesterol with oxidized phospholipid species in lipid bilayers. Soft Matter 10, 639–947.
Kinnunen, P.K.J., Kaarniranta, K., Mahalka, A.K., 2012. Protein-oxidized phospholipid interactions in cellular signaling for cell death: from biophysics to clinical correlations. Biochim. Biophys. Acta 1818, 2446–2455.
Koppaka, V., Axelsen, P.H., 2000. Accelerated accumulation of amyloid β proteins and oxidatively damaged lipid membranes. Biochemistry 39, 10011–10016.
Kucerka, N., Liu, Y., Chu, N., Petrache, H.I., Tristram-Nagle, S., Nagle, J.F., 2005. Structure of fully hydrated fluid phase DMPC and DLPC lipid bilayers using X-ray scattering from oriented multilamellar arrays and from unilamellar vesicles. Biophys. J. 88, 2626–2637.
Lai, C.C., Yang, S.H., Finlayson-Pitts, B.J., 1994. Interactions of monolayers of unsaturated phosphocholines with ozone at the air–water interface. Langmuir 10, 4637–4644.
Li, X.-M., Momsen, M.M., Smaby, J.M., Brockman, H.L., Brown, R.E., 2001. Cholesterol decreases the interfacial elasticity and detergent solubility of sphingomyelins. Biochemistry 40, 5954–5963.
Lis, M., Wizert, A., Przybylo, M., Langner, M., Swiatek, J., Jungwirth, P., Cwiklik, L., 2011. The effects of lipid oxidation on the water permeability of phospholipids bilayers. Phys. Chem. Chem. Phys. 13, 17555–17563.
MacCallum, J.L., Drew Bennet, W.F., Tieleman, D.P., 2008. Distribution of amino acids in a lipid bilayer from computer simulations. Biophys. J. 94, 3393–3404.
Matti, V., Säily, J., Ryhänen, S.J., Holopainen, J.M., Borocci, S., Mancini, G., Kinnunen, P.K.J., 2001. Characterization of mixed monolayers of phosphatidylcholine and a dicationic Gemini surfactant SS-1 with a Langmuir balance: effects of DNA. Biophys. J. 81, 2135–2143.
Mattila, J.-P., Sabatini, K., Kinnunen, P.K.J., 2008. Interaction of cytochrom *c* with 1-palmitoyl-2-azelaoyl-*sn*-glycero-3-phosphocholine: evidence for acyl chain reversal. Langmuir 24, 4157–4160.
Megli, F.M., Sabatini, K., 2003. Respiration state IV-generated ROS destroy the mitochondrial bilayer packing order in vitro. An EPR study. FEBS Lett. 550, 185–189.
Megli, F.M., Sabatini, K., 2004. Mitochondrial phospholipid bilayer structure is ruined after liver oxidative injury in vivo. FEBS Lett. 573, 68–72.
Megli, F.M., Rosso, L., Sabatini, K., 2005. Oxidized phospholipids induce phase separation in lipid vesicles. FEBS Lett. 579, 4577–4584.
Nagle, J.F., et al., 2013. General discussion. Faraday Discuss. 161, 563–589.
Nepomuceno, M.F., Alonso, A., Pereira-da-Silva, L., Tabak, M., 1997. Inhibitory effect of dipyridamole and its derivatives on lipid peroxidation in mitochondria. Free Radic. Biol. Med. 23, 1046–1054.
O'Donnel, V.B., 2011. Mass spectrometry analysis of oxidized phosphatidylcholine and phosphatidylethanolamine. Biochim. Biophys. Acta 1811, 818–826.
Orsi, M., Michel, J., Essex, J.W., 2010. Coarse-grain modelling of DMPC and DOPC lipid bilayers. J. Phys. Condens. Matter 22, 155106–155120.
Parkkila, P., Stefl, M., Olzynska, A., Hof, M., Kinnunen, P.K.J., 2015. Phospholipid lateral diffusion in phosphatidylcholine-sphingomyelin-cholesterol monolayers; effects of oxidatively truncated phosphatidylcholines. Biochim. Biophys. Acta 1848, 167–173.
Roiter, Y., Ornatska, M., Rammohan, A.R., Balakrishnan, J., Heine, D.R., Minko, S., 2009. Interaction of lipid membrane with nanostructured surfaces. Langmuir 25, 6287–6299.
Sabatini, K., Mattila, J.-P., Megli, F.M., Kinnunen, P.K.J., 2006. Characterization of two oxidatively modified phospholipids in mixed monolayers with DPPC. Biophys. J. 90, 4488–4499.

Singer, S.J., Nicolson, G.L., 1972. The fluid mosaic model of the structure of cell membranes. Science 175, 720–731.
Uhlson, C., Harrison, K., Allen, C.B., Ahmad, S., White, C.W., Murphy, R.C., 2002. Oxidized phospholipids derived from ozone-treated lung surfactant extract reduce macrophage and epithelial cell viability. Chem. Res. Toxicol. 15, 896–906.
Volinsky, R., Kinnunen, P.K.J., 2013. Oxidized phosphatidylcholines in membrane-level cellular signaling: from biophysics to physiology and molecular pathology. FEBS J. 280, 2806–2816.
Volinsky, R., Cwiklik, L., Jurkiewicz, P., Hof, M., Jungwirth, P., Kinnunen, P.K.J., 2011. Oxidized phosphatidylcholines facilitate phospholipid flip-flop in liposomes. Biophys. J. 101, 1376–1384.
Volinsky, R., Paananen, R., Kinnunen, P.K.J., 2012. Oxidized phosphatidylcholines promote phase separation of cholesterol-sphingomyelin domains. Biophys. J. 103, 247–254.
Wallgren, M., Lidman, M., Pham, Q.D., Cyprych, K., Gröbner, G., 2012. The oxidized phospholipid PazePC modulates interactions between Bax and mitochondrial membranes. Biochim. Biophys. Acta 1818, 2718–2724.
Wallgren, M., Beranova, L., Pham, Q.D., Linh, K., Lidman, M., Procek, J., Cyrpych, K., Kinnunen, P.K.J., Hof, M., Gröbner, G., 2013. Impact of oxidized phospholipids on the structural and dynamic organization of phospholipid membranes: a combined DSC and solid state NMR study. Faraday Discuss. 161, 499–513.